Int J Adv Manuf Technol (2012) 59:583–591
DOI 10.1007/s00170-011-3538-5

ORIGINAL ARTICLE

Microstructural characterization and mechanical properties of functionally graded PA12/HDPE parts by selective laser sintering

Janaina Lisi Leite · Gean Victor Salmoria · Rodrigo A. Paggi · Carlos Henrique Ahrens · Antonio Sérgio Pouzada

Received: 30 June 2010 / Accepted: 20 July 2011 / Published online: 20 August 2011

Abstract The use of selective laser sintering in the production of functional gradient materials offers advantages, as freeform construction and localized control of the composition and process parameters, compared to other rapid manufacturing processes. In this work, selective laser sintering was used for manufacturing three-dimensional parts in functionally graded polymer blends based on polyamide 12 and high-density polyethylene with gradient composition in two directions (*Y* and *Z*). Test specimens were prepared in PA12/HDPE ratios of 0/100, 20/80, 50/50, 80/20 and 100/0 (*w*/*w*). These specimens were assessed in terms of density, microstructure by scanning electron microscopy and polarized light microscopy and mechanical performance by DMA. The sintered binary blend systems with composition gradient showed microstructure and properties variation as function of the blend compositions. The results demonstrated the potential of selective laser sintering to manufacture advanced polymeric functional gradient material parts.

Keywords Functionally gradient material · PA12/HDPE blend · Selective laser sintering

Electronic supplementary material The online version of this article (doi:10.1007/s00170-011-3538-5) contains supplementary material, which is available to authorized users.

G. V. Salmoria · R. A. Paggi · C. H. Ahrens
Laboratorio CIMJECT, Departamento de Engenharia Mecânica,
Universidade Federal de Santa Catarina,
88040-900 Florianópolis, Santa Catarina, Brazil

A. S. Pouzada (✉)
Institute for Polymers and Composites/I3N,
University of Minho,
4800-058 Guimarães, Portugal
e-mail: asp@dep.uminho.pt

J. Lisi Leite
Mestrado Profissional em Engenharia Mecânica,
Instituto Superior Tupy - Sociedade Educacional
de Santa Catarina (SOCIESC),
Joinville, SC 89206-001, Brazil
e-mail: lisileite@yahoo.com.br

1 Introduction

The concept of functionally graded material (FGM) aims at designing composite materials characterised by continuous variation of the properties and obtained by varying the composition in the part [1–3]. In recent years, numerous applications for FGM have been identified in the electrical, photoelectrical, mechanics, aerospace, automobile, medical or chemical areas [4–6]. The FGM performance is mainly dependent on the phase distribution of the constituent materials, this being tailored to achieve specific requirements and properties of the final part [7].

The composition gradient is designed to satisfy specific requirements or functions of the component in service, that is, the FGM can improve its performance through the controlled variation of properties associated with the varying composition [8]. The manufacture of this type of composite components can be made by various techniques and methods that are continuously under development, e.g. die compaction of layer, wet powder spraying, slurry dipping and slip casting, centrifugal powder forming, centrifugal casting, controlled mould filling or infiltration process. Nevertheless, most of the reported solutions are limited to one-dimensional FGM in simple shapes [4, 9]. Rapid prototyping is being increasingly used for FGM

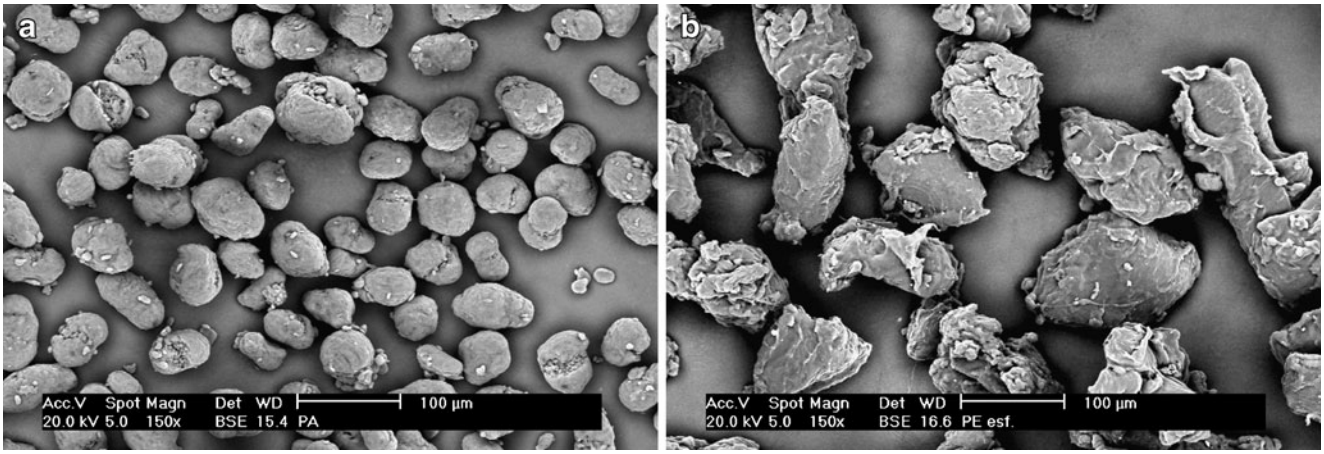

Fig. 1 Micrographs of **a** PA12 and **b** HDPE particles

because these layered manufacturing techniques can produce freeform geometries with a variety of materials (polymers, metals and ceramics) [10, 11]. With the technique of selective laser sintering (SLS), powder particles are fused or heat sintered together layer by layer using an infrared laser, which is very convenient for FGM manufacturing [12–14].

The availability of commercial polymers for SLS is limited, which reduces the options for the selection of the optimum material for the manufacturing of the parts. Polymeric blends and composites have being seen as an interesting alternative for SLS parts with variable composition throughout the part [15–18]. The polyamide/polyolefin blends are attractive because of the specific properties of each polymer. Polyamides (PA) exhibit good resistance to solvents, high strength and wear resistance. High-density polyethylene (HDPE) has excellent low temperature toughness, low cost and excellent tribological properties [19, 20].

In this work that follows the research published elsewhere [21], the fabrication of polymeric FGM by SLS was investigated using a binary PA12/HDPE blend system. The specimens were fabricated in variable weight by weight compositions, and analysed in terms of microstructure and mechanical properties by microscopy and dynamic mechanical analyses. The functionally graded PA12/HDPE blends were manufactured as planar parts by SLS. The property gradient was established across the thickness (*Z*-direction) and along one of the plane directions (*Y*-direction).

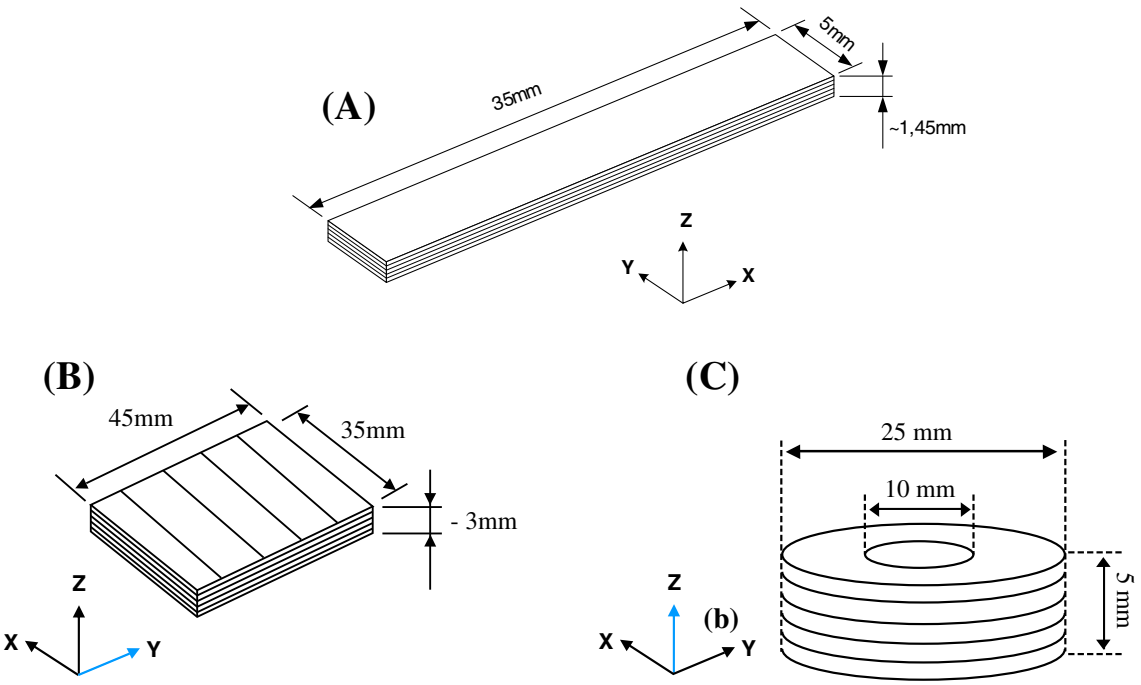

Fig. 2 **a** Bar of sintered mono-material, **b** plate with functionally graded PA12/HDPE composition in the *Y*-direction, **c** circular part with functionally graded PA12/HDPE composition in the *Z*-direction

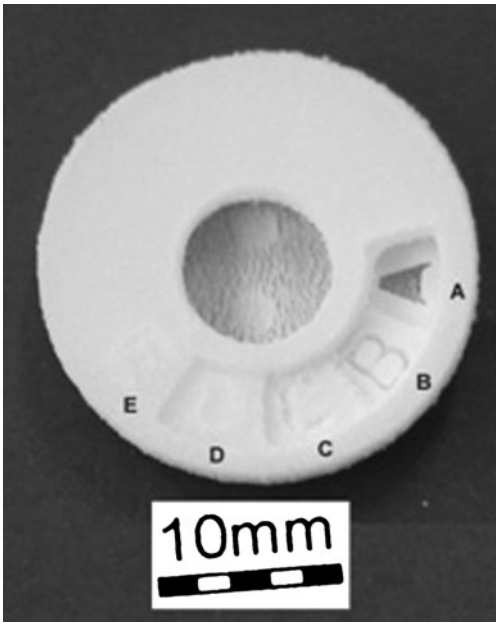

Fig. 3 Cylindrical part (type C) features a material gradient in the SLS build *Z*-direction

2 Experimental

2.1 Materials

The polymers used in this study were a commercial PA 12 specific grade for SLS (PA2200 from EOSINT, Germany), with an average particle size of around 60 μm and an HDPE UV-additivated grade with melt flow rate of 7.5 g/600 s (190°C/2.16 kg) (HD7555 from Ipiranga, Brazil) ground to particle size in the range from 80 to 200 μm (Fig. 1).

2.2 Test parts

Three test parts were considered (Fig. 2): (1) parallelepiped bar (35×5×1.4 mm) for mechanical characterisation of the various compositions, (2) plate (45×35×3 mm) for binary parts with a composition gradient in the *Y*-direction (i.e. the plane of each layer), and (3) cylindrical part with surface features (∅25×5 mm) to obtain a gradient in the *Z*-direction (i.e. in the build direction).

The type of FGM solution with constant characteristics across thickness and variable property in the plane (type B) may be applied in parts where the stiffness and toughness of the processed material are important parameters. The cylindrical part (type C) features a material gradient in the SLS build direction and one of the produced parts is shown in Fig. 3. This component can be seen as a bushing disc where one side has to be hard and stiff to allow secure fixation or have self-lubricating properties conferred to by the PA12 phase and the other side has to be flexible to allow better adjustment with adjacent components.

The blends were prepared by physical mixing in a Y-mixer, with PA12/HDPE proportions of 100/0, 80/20, 50/50, 20/80 and 0/100 (*w*/*w*).

The test parts were sintered with a prototype SLS equipment designed and built at the Federal University of Santa Catarina [22]. The apparatus works with 10 W RF-excited CO_2 laser with wavelength of 10.6 μm. The laser beam diameter used in the production of the parts was of 250 μm. Due to the characteristics of the powder feed system of the equipment it is not possible laser sintering of 3D functionally graded materials. The processing parameters adopted for sintering the various compositions were adjusted previously to produce parts with overall acceptable quality, and are listed in Table 1. In particular, the laser power was adjusted to give the best particle cohesion and mechanical properties. It is noteworthy that the powder bed temperature rise for PA12/HDPE (100/0) was found adequate to cope with the higher melting point of PA 12 (184°C) compared with the HDPE (approximately 130°C). In every case, the layer thickness was kept constant at 150 μm.

The plate with functionally graded composition in the *Y*-direction (type B) was manufactured by automatic dispersion of the blend mixture in the *Y*-direction graded layer before sintering due to the SLS powder delivery device. Intermediate parameters used for the single blend specimen were applied to produce plate FGM.

Table 1 Sintering parameters

Sample	PA12/HDPE (%)	Laser power (W)	Energy density (MJ/m^2)	Scan speed (mm/s)	Powder bed temperature (°C)	Chamber temperature (°C)
A	100/0	3.33	0.299	44.5	140	110
	80/20	4.05	0.364		100	
	50/50	4.50	0.404		100	
	20/80	4.32	0.388		100	
	0/100	4.95	0.445		100	
B	Gradient *Y*-direction	4.50	0.404		100	
C	Gradient *Z*-direction	[a]	[a]	[a]	[a]	[a]

[a] The sintering parameters were set depending on the composition of each layer, identical to those used for the samples A

The cylindrical part with functionally graded composition in the *Z*-direction (type C) was built in discrete layers by the powder supply device semi-automatic, using sintering parameters according to the blend composition as in Table 1. As the SLS process proceeded, the powder supply device deposited material of a gradually changing composition on the part. The processing parameters for each composition were changed synchronously. This technique created multi-

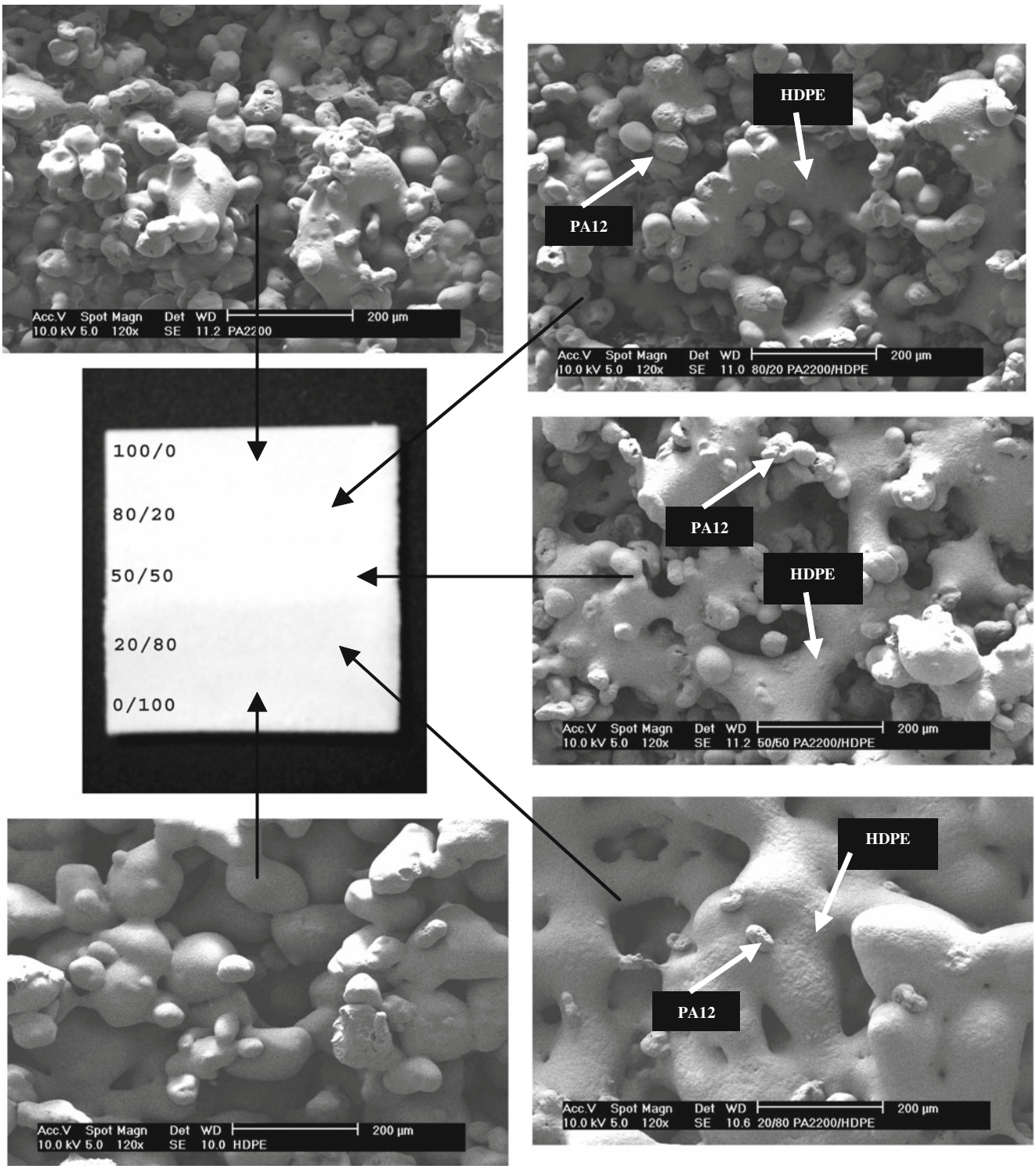

Fig. 4 Topography of the PA12/HDPE part with functionally graded composition in the *Y*-direction. The SEM micrographs show the surfaces corresponding to the various PA12/HDPE composition regions

Table 2 Density data of PA12/HDPE sintered compositions

PA12/HDPE composition	Bulk density (Mg m^{-3})	Theoretical density (Mg m^{-3})	Porosity (%)
100/0	0.56	1.02	45
80/20	0.62	1.00	38
50/50	0.68	0.98	31
20/80	0.66	0.96	31
0/100	0.55	0.95	42

layer FGM parts in which the material gradient was oriented along the build direction, i.e. in *Z*-direction.

2.3 Testing

2.3.1 Physical testing

Sintered specimens of PA12, HDPE and each of the PA12/HDPE blends were characterised in terms of density which was determined by picnometry.

The degree of porosity of the test pieces was assessed indirectly through the apparent density. The theoretical density of the blends was calculated using the law of mixtures [23]:

$$\rho_{\text{blend}} = f_{\text{HDPE}} \times \rho_{\text{HDPE}} + (1 - f_{\text{HDPE}}) \times \rho_{\text{PA12}} \quad (1)$$

where ρ_{blend}, ρ_{HDPE} and ρ_{PA12} are the blend, HDPE and PA12 densities, respectively, and f_{HDPE} and f_{PA12} are the HDPE and PA12 fractions in the blend, respectively.

2.3.2 Microscopy

The microstructures of the plate with functionally graded composition in the *Y*-direction were analysed by scanning electron microscopy (SEM) using Philips XL30 equipment. The specimens were previously coated with gold using a Bal-Tec Sputter Coater SCD005.

The through-thickness morphology of the circular disc with functionally graded composition in the *Z*-direction was analysed by polarized light microscopy. The morphology of these parts was observed on thin-sliced sections of 10 μm obtained with a Leitz 1401 microtome, using a polarized light microscope Olympus BH-2 (Tokyo, Japan).

2.3.3 Mechanical testing

The mechanical analysis of the blends was carried out using the sintered bar (Fig. 2a) in a dynamic mechanical analyser DMA Q800 (TA Instruments, USA). The tests were carried out in the single cantilever mode with constant strain rate, at 30°C and a loading rate of 2 N/min up to a maximum of 18 N.

3 Results and discussion

3.1 FGM topography

The surface of the PA12/HDPE functionally graded plate with composition varying in the *Y*-direction is shown in the SEM micrographs of Fig. 4. The stepwise changes in composition and good bonding in the composition transitional interface regions are visible. These results indicate that FGM of PA12 and HDPE with step increments of 20% and 30% of the component fractions in one direction can be successfully produced in a single uninterrupted SLS process run.

The expected immiscibility of the polymer phases is confirmed by the SEM observations, the two phases being clearly visible in the surface of the part, as it can be observed in the micrographs in Fig. 4. The morphology throughout the surface of the PA12/HDPE FGM plate is heterogeneous with co-continuous and disperse phases depending on the local content of HDPE. The weak adherence of the PA12 particles to the HDPE phase is due to their different molecular polarities. The porosity also changes with the local composition. There is a gradual variation in the distribution of interconnected pores with the average size being related to the particle size and shape of the powder components. The HDPE domains reveal a higher degree of sintering and reduced porosity, with the processing parameters used in this study, the individual particles being connected by extensive neck formations.

Specific features are associated to the various regions in the FGM plate. In the 80/20 PA12/HDPE region, the formation of a PA12 and HDPE co-continuous phase occurred, with adherent particles of PA12. These PA12 particles form due to the earlier solidification determined by the higher melting temperature (184°C) in comparison with the HDPE (approximately 135°C). The pore size in this specimen is smaller than 200 μm. In the region where the 50/50 composition was sintered, a large co-continuous HDPE phase was formed and some particles of PA12 are seen adhering to the HDPE matrix. The porosity in this region is lower than in the 80/20 region, as a consequence of the larger co-continuous HDPE phase. During the microstructure formation the HDPE keeps its flowability differently from PA12 that is already solidified at that stage.

Table 3 Dimension values and deviation of sintered FGM disc

	Dimension in the model (mm)	Dimension in the final part (mm)	Shrinkage (%)
Inner diameter	10.0	8.92±0.12	10.80
Outer diameter	25.0	24.53±0.09	1.88
Height	5.0	4.30±0.21	14.10

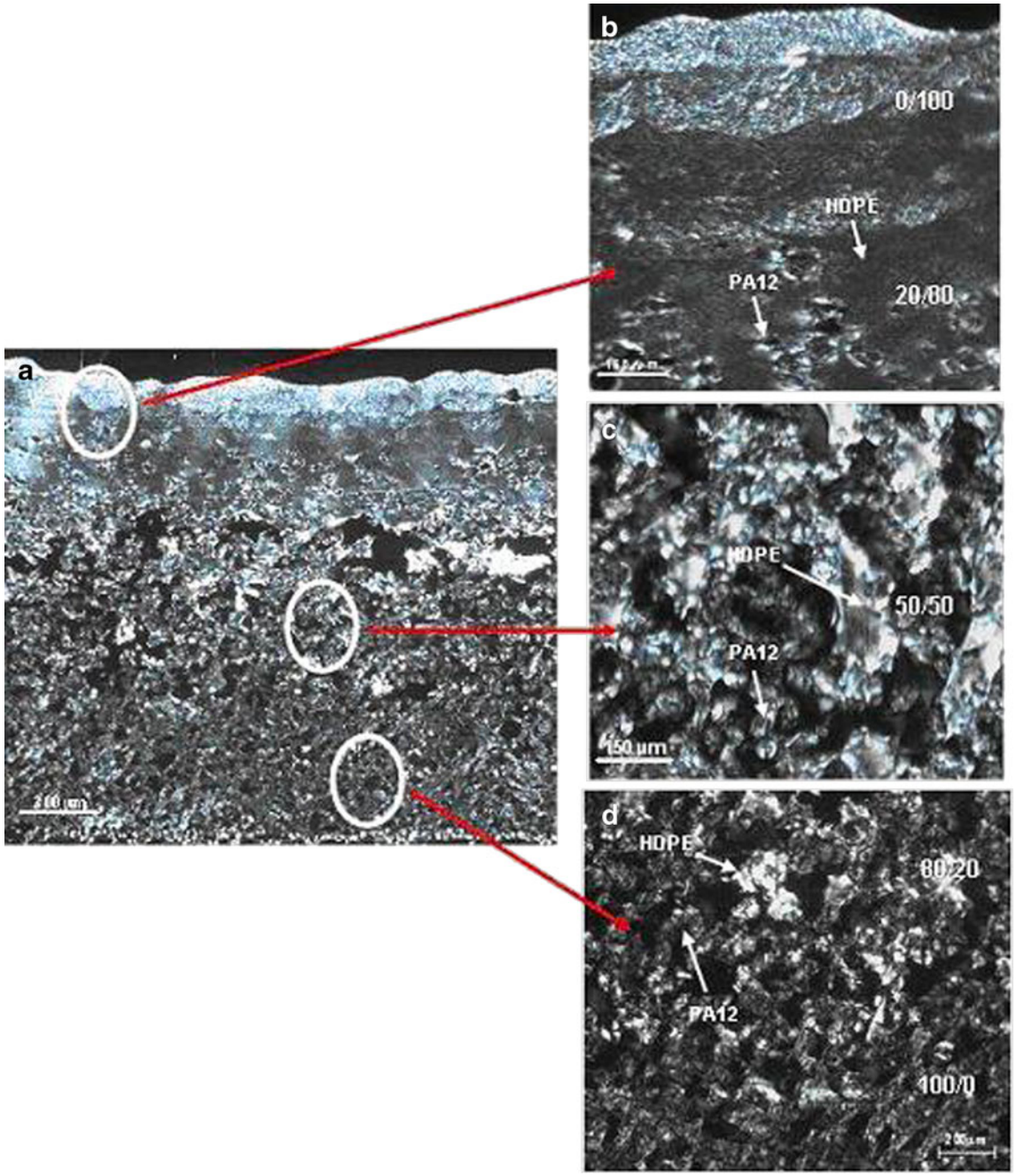

Fig. 5 Microstructure of the PA12/HDPE graded composition in the *Z*-direction: **a** whole section, **b** 0/100 and 20/80 zones, **c** 50/50 zone and **d** 80/20 and 100/0 zones

This environment facilitates the coalescence of HDPE particle and the consolidation of the co-continuous phase. Finally, at the surface of 20/80 PA12/HDPE, a dense HDPE matrix is formed and particle union through neck formation and coalescence is observable. This microstructure, where fewer PA12 are clearly identified, is similar to the single HDPE phase that was formed from a molten polymer with higher viscosity than the PA12.

The surface micrographs of the richer HDPE regions (100% and 80%) depict larger pores in comparison with the single PA12. The HDPE phase has a sintered matrix pattern, which differs from the other blends where PA12 is predominant (50/50 and 20/80 composition). This is attributable not only to the lower laser energy absorption shown by this polymer but also to the smaller size of the PA12 particles.

The complex effects of the laser powder sintering process and the blend composition on the microstructure formation (extent of sintering, co-continuity of the phases and porosity) have a determinant role in the properties of

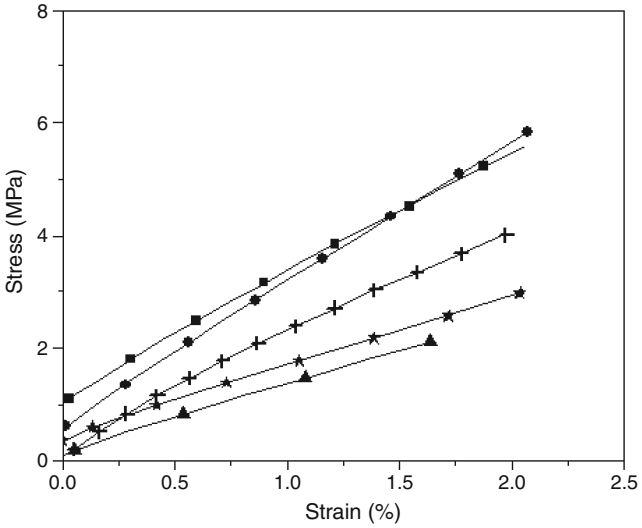

Fig. 6 Stress versus strain curves for sintered PA12/HDPE blends: (*black squares*) 100/0, (*black circles*) 80/20, (*plus sign*) 50/50, (*stars*) 20/80, (*black triangle*) 0/100

the FGM parts. The determination of the bulk density and its comparison with the theoretical density determined using a simple rule of mixtures provides information on the likely porosity of the sintered parts. In Table 2, density data for sintered PA12, HDPE and various PA12/HDPE compositions are given. The single PA12 and HDPE sintered specimens have higher porosity than the PA12/HDPE compositions (Fig. 4). The slightly better compacity of the PA12/HDPE compositions illustrates the beneficial effect of the presence of particles of different materials in the FGM.

3.2 Shrinkage

In this work, the circular part with functionally graded PA12/HDPE composition in the *Z*-direction (type C) was considered for the analysis of the shrinkage and the internal microstructure.

The dimensions of the sintered FGM discs were determined and compared to the CAD input dimensions of the model. The data in Table 3 provides information on the shrinkage that is associated to the process. The larger shrinkage of 14% corresponds to the free shrinkage across thickness in the build direction. In the diametrical direction, there is a substantial difference in the inner diameter (approximately 2%) and the outer diameter (11%). This effect is a result from the restricted shrinkage in the inner zone of the part.

It is interesting to note that the shrinkage observed on sintered FGM parts of semi-crystalline materials is completely different from that already reported when producing similar parts on amorphous PMMA/HIPS blends [24].

3.3 Internal microstructure

The internal microstructure that is important for the mechanical behaviour and the barrier properties of the FGM parts was observed in thin sections. The cross-section micrograph of the disc in the zone E is shown in Fig. 5.

The polarized light micrographs can provide objective information on the developed microstructure and also on the dispersion of the phases. The immiscibility of the polymer phases is confirmed in the details of the morphology across the thickness shown in Fig. 5. Two semi-crystalline phases depicting the typical morphologies of HDPE and PA12 in the layered microstructure observed by polarized light microscopy across the *Z*-direction. The very fine spherulitic microstructure of HDPE and the coarser one of PA12 are clearly identifiable.

The PA12 regions are dense and show as disperse inclusions the HDPE domains. Co-continuous phases are present in the region corresponding to the 50/50 blend. Voids are also observed in this region, resulting probably from the different particle size and solidification and shrinkage of HDPE in the already solidified PA12 phase.

3.4 Mechanical performance

The application of a model based in the law of mixtures [23], as previously for the degree of porosity, is used to predict the mechanical properties of the blends, assuming that the specimens are void-free and there is complete coupling between the phases [24].

The mechanical behaviour of the specimens under low strain (less than 2%) is shown in Fig. 6. These data were obtained by DMA at constant strain rate of 2 Nm^{-1} in

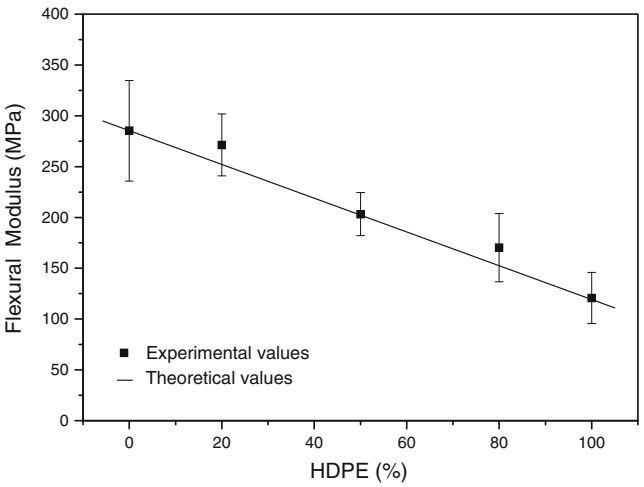

Fig. 7 Theoretical and experimental values of flexural modulus to PA12/HDPE blends as a function of HDPE content

single-cantilever flexural testing. The stress–strain behaviour of the blends under low strain shows that an increase in the HDPE fraction leads to a reduction in their stiffness or flexural modulus.

The experimental flexural modulus data for the PA12/HDPE blends are plotted in Fig. 7 against the values predicted using the law of mixtures. The graph clearly shows a decrease in the modulus with increasing the HDPE content. This reduction in the stiffness follows quite closely the expectations from the rule of mixtures and illustrates the softening effect of the HDPE phase that has a much lower modulus than PA12. Some variation in the experimental data with respect to the predictions may result from the void fraction not being considered.

4 Conclusions

In this work, properties of binary PA12/HDPE parts with functionally graded composition in the *Y* and *Z*-directions processed by SLS were analysed.

The fabrication of FGM parts with property gradient in the build direction and in one of the platform directions was made by SLS. For this purpose, the recoater of the equipment deposited material with gradually changing composition on the building platform as the stacked powders of different compositions were incrementally consumed.

The sintered PA12/HDPE parts, besides continuous HDPE and PA12 domains, showed the occurrence of variable percentage of pores, depending on the blend composition and the particle size. The topography of the sintered parts revealed features that are related to the composition and are attributable to the viscosities of the molten polymers and their melt temperatures. The PA12 phase tends to appear as individualised particles, whereas the HDPE forms a co-continuous phase where the PA12 is segregated in quasi-spherical particles.

The analysis by light microscopy of a PA12/HDPE FGM part revealed a gradually varying microstructure across its thickness. It was also possible to confirm the existence of voids in the mass of the sintered part that may have resulted from the different size of the particles and also the very different crystallisation temperatures.

The mechanical properties depend mostly from the PA12/HDPE composition and can be approximately predicted by application of the law of mixtures. The flexural moduli of the PA12/HDPE blends showed that a higher content of the tougher component, i.e. HDPE, led to a decrease in the flexural modulus, reducing the rigidity of the blends.

The manufacture of polymer blend parts with composition gradient by SLS showed that different microstructures can be obtained depending on the composition of blends, enabling the manufacture of components with different properties and functions and permitting the development of new area applications using rapid manufacture technologies.

Acknowledgements The authors thank FAPESC, CNPq and FINEP, in Brazil, for the financial support, and the Covenant Brazil-Portugal supported by CAPES in Brazil and FCT in Portugal. The suggestions of Dr. Maria Jovita Oliveira at the University of Minho regarding the light microscopy analysis are also acknowledged.

References

1. Wen B, Wu G, Yu J (2004) A flat polymeric gradient material: preparation, structure and property. Polymer 45:3359–3365
2. Edwards KL (2002) Linking materials and design: an assessment of purpose and progress. Mater Des 23:255–264
3. Shishkovsky I (2001) Synthesis of functional gradient parts via RP methods. Rapid Prot J 7:207–211. doi:10.1108/13552540110402908
4. Bernard A, Taillandier G, Karunakaran KP (2009) Evolutions of rapid product development with rapid manufacturing: concepts and applications. Int J Rapid Manuf 1:3–18
5. Petrovic V, Gonzalez JVH, Ferrando OJ, Gordillo JD, Puchades JRB, Griñan LP (2010) Additive layered manufacturing: sectors of industrial application shown through case studies. Int J Prod Res. doi:10.1080/00207540903479786
6. Ning N-Y, Zhu Y-B, Zhang X-Q, He Z-K, Fu Q (2007) A new technique for preparing polyethylene/polystyrene blends with gradient structure. J Appl Polym Sci 105:2737–2743
7. Jin G, Takeuchi M, Honda S, Nishikawa T, Awaji H (2005) Properties of multilayered mullite/Mo functionally graded materials fabricated by powder metallurgy processing. Mater Chem Phys 89:238–243
8. Su WN (2002) Layered fabrication of tool steel and functionally graded materials with a Nd: YAG Pulsed Laser. PhD Thesis. Loughborough University, Loughborough, UK
9. Kieback B, Neubrand A, Riedel H (2003) Processing techniques for functionally graded materials. Mater Sci Eng 362:81–106
10. Hopkinson N, Dickens P (2003) Analysis of rapid manufacturing—using layer manufacturing processes for production. Proc IME C J Mech Eng Sci 217:31–39
11. Calder N Rapid manufacturing of functional materials, in TCT2001 Conference2001: Manchester
12. Kumar S, Kruth JP (2010) Composites by rapid prototyping technology. Mater Des 31:850–856
13. Chung H, Das S (2008) Functionally graded Nylon-11/silica nanocomposites produced by selective laser sintering. Mater Sci Eng 487:251–257
14. Caulfield B, McHugh PE, Lohfeld S (2007) Dependence of mechanical properties of polyamide components on build parameters in the SLS process. J Mater Process Tech 182:477–488
15. Yan C, Shi Y, Yang J, Liu J (2011) Investigation into the selective laser sintering of styrene–acrylonitrile copolymer and postprocessing. Int J Adv Manuf Technol 51:973–982
16. Chung H, Das S (2006) Processing and properties of glass bead particulate-filled functionally graded Nylon-11 composites produced by selective laser sintering. Mater Sci Eng 437:226–234

17. Chiu WK, Yu KM (2008) Multi-criteria decision-making determination of material gradient for functionally graded material objects fabrication. Proc IME B J Eng Manufact 222:293–307
18. Salmoria GV, Paggi RA, Lago A, Beal VE (2009) Functionally graded PA12/MWCNTs composite fabricated by SLS to aerospace applications: mechanical and electrical behavior. In: Bártolo PJ (ed) Innovative developments in design and manufacturing—advanced research in virtual and rapid prototyping. Taylor and Francis, London, pp 55–60
19. Jiang C, Filippi S, Magagnini P (2003) Reactive compatibilizer precursors for LDPE/PA6 blends. II: maleic anhydride grafted polyethylenes. Polymer 44:2411–2422
20. Palabiyik M, Bahadur S (2000) Mechanical and tribological properties of polyamide 6 and high density polyethylene polyblends with and without compatibilizer. Wear 246: 149–158
21. Salmoria GV, Leite JL, Ahrens CH, Lago A, Pires ATN (2007) Rapid manufacturing of PA/HDPE blend specimens by selective laser sintering: microstructural characterization. Polym Test 26:361–368
22. Salmoria GV, Leite JL, Ahrens CH, Paggi RA, Lago A (2007) Manufacture by selective laser sintering of functionally graded PA 6/PA 12 components with applications in antifriction materials. In: Bártolo PJ (ed) Virtual and rapid manufacturing—advanced research in virtual and rapid prototyping. Taylor and Francis, London, pp 313–317
23. Fan Z, Tsakiropoulos P, Miodownik AP (1994) A generalized law of mixtures. J Mater Sci 29:141–150. doi:10.1007/bf00356585
24. Leite JL, Salmoria GV, Paggi RA, Ahrens CH, Pouzada AS (2010) A study on morphological properties of laser sintered functionally graded blends of amorphous thermoplastics. Int J Mat Prod Tech 39:205–222